

Sorption Properties of Crystalline Molecular Sieve $\text{AlPO}_4\text{-5}$ V. R. CHOUDHARY,¹ D. B. AKOLEKAR, A. P. SINGH, AND S. D. SANSARE*Chemical Engineering Division, National Chemical Laboratory, Pune 411 008, India*

Received March 25, 1987; revised November 20, 1987

The sorption capacity of a number of sorbates, viz. alcohols and hydrocarbons, and the isotherms of sorption of methanol, *n*-hexane, and benzene in $\text{AlPO}_4\text{-5}$ at 313 K were measured by gravimetric technique. The isotherms of sorption of *n*-hexane, cyclohexane, benzene, and pyridine in the $\text{AlPO}_4\text{-5}$, at higher temperatures (523–673 K) were determined by the GC peak maxima method. The isosteric heats of sorption of these sorbates at different sorbate loadings were obtained from the isotherm data. The heat of sorption near zero sorbate loading was determined separately by the GC pulse technique in the temperature range 523–673 K. The sorption capacities of $\text{AlPO}_4\text{-5}$ for the sorbates, differing widely in their dipole moments and critical molecular sizes, have been found to be nearly the same (about $0.14 \text{ cm}^3 \cdot \text{g}^{-1}$). The sorption of methanol, *n*-hexane, and benzene at 313 K occurs by the volume filling mechanism and the total volume of the sorption space in $\text{AlPO}_4\text{-5}$ has been found to be about $0.14 \text{ cm}^3 \cdot \text{g}^{-1}$. The sorption of *n*-hexane, cyclohexane, benzene, and pyridine at the higher temperatures follows the Freundlich isotherm. The influence of sorbate loading on the isosteric heat of sorption of benzene is very weak but the influence in the case of the other sorbates is very strong, particularly at the higher sorbate loadings. With the increase in the sorbate loading, the heat of sorption of *n*-hexane and pyridine increases and that of cyclohexane decreases. The heat of sorption of pyridine is much higher than that of the other sorbates. The values of the heat of sorption of *n*-hexane, cyclohexane, and benzene at near zero sorbate loading, obtained by the two methods, are very close to each other, and there is very good agreement between the heats of sorption obtained by the two methods. Analysis of the entropy change data for the high-temperature sorption reveals that the sorption of all the sorbates is mobile; the sorption of *n*-hexane at lower sorbate loading, in particular, and that of cyclohexane and benzene are "supermobile." However, in the case of sorption of *n*-hexane at higher sorbate loadings and pyridine, the sorbed molecules lose some of their rotational degrees of freedom.

© 1988 Academic Press, Inc.

INTRODUCTION

$\text{AlPO}_4\text{-5}$, a zeolite-like aluminophosphate introduced recently by Wilson *et al.* (1, 2), has a novel three-dimensional structure with one-dimensional cylindrical channels (formed by 12-membered rings) of uniform cross section (pore diameter = 0.8 nm) oriented parallel to the *c*-axis, which is crystallographically polar (3). Because of its neutral framework, it does not contain framework cations. However, it contains weak acid sites, both Lewis and protonic (4, 5). It is moderately hydrophilic and has interesting water sorption properties (2). Water sorption on $\text{AlPO}_4\text{-5}$ (at 297 K) follows a Type V isotherm shape, unusual for

microporous solids and zeolites. A knowledge of the sorption properties of $\text{AlPO}_4\text{-5}$ for various organic compounds is of great interest. Very little, however, is known about these properties, as only a few related studies have been carried out so far. Wilson *et al.* (2) have measured the sorption isotherms of water (at 297 K) and oxygen (at 90 K) on $\text{AlPO}_4\text{-5}$. Choudhary and Akolekar (5) have investigated the chemisorption and temperature-programmed desorption (TPD) of pyridine on $\text{AlPO}_4\text{-5}$.

In our earlier studies, the site energy distribution and catalytic properties of $\text{AlPO}_4\text{-5}$ (5) and the influence of thermal, hydrothermal, and acid–base treatments on its structural stability and surface and catalytic properties (6) have been reported. The objective of the present investigation was to

¹ To whom all correspondence should be addressed.

determine the sorption capacity of $\text{AlPO}_4\text{-5}$ for various hydrocarbons and alcohols, to study its sorption properties at lower and higher temperatures, and to investigate the thermodynamics of sorption of *n*-hexane, benzene, and pyridine in the aluminophosphate.

EXPERIMENTAL

The $\text{AlPO}_4\text{-5}$ ($\text{Al/P} = 1.03$) was obtained from $\text{Pr}_3\text{N-AlPO}_4\text{-5}$ by heating it in air at 813 K for 12 h, to remove the organic template from it. The synthesis of $\text{Pr}_3\text{N-AlPO}_4\text{-5}$ has been described previously (5). The $\text{AlPO}_4\text{-5}$ was pressed without any binder and crushed to particles of about 0.2 mm in size. The size of the hexagonal rod-like crystals of the aluminophosphate was about 22 μm . A detailed characterization of the aluminophosphate for its crystalline nature, crystal size and morphology, acidity, and site energy distribution is given in our earlier paper (5).

The sorption capacity of $\text{AlPO}_4\text{-5}$ for water, hydrocarbons (viz. *n*-hexane, cyclohexane, benzene, *p*-xylene, *o*-xylene, and isooctane), and alcohols (viz. methanol, ethanol, and *n*-butanol) was determined gravimetrically by passing the sorbate vapors along with helium (flow rate, about 100 $\text{cm}^3 \cdot \text{min}^{-1}$) at a relative pressure of 0.4 over the aluminophosphate (0.5 g) kept in a glass cell (capacity, 10 cm^3) at 313 K until the sorption equilibrium was established. The relative pressure (p/p_s) is the ratio of the partial pressure (p) of the sorbate in the sorbate/helium mixture to the saturated vapor pressure of the sorbate at the sorption temperature. The glass cell was provided with Teflon stopcocks at the inlet and the outlet and could be detached from the flow system for direct weighing on an electronic analytical balance, without exposing the sorbate-sorbent system to the atmosphere. Before the sorption measurement, the aluminophosphate was pretreated *in situ* in a flow of pure helium (flow rate, 100 $\text{cm}^3 \cdot \text{min}^{-1}$) at 623 K for 2 h.

Isotherms of sorption of *n*-hexane, benzene, and methanol in the aluminophosphate at 313 K were obtained by measuring gravimetrically the sorption of the individual sorbate at different relative pressures ($p/p_s = 0 - 0.4$) by the procedure described above.

The irreversible sorption of *n*-hexane, cyclohexane, and benzene in $\text{AlPO}_4\text{-5}$ was measured by the GC methods based on TPD under chromatographic conditions (7) and stepwise thermal desorption (8).

Isotherms of reversible sorption of *n*-hexane, cyclohexane, benzene, and pyridine in $\text{AlPO}_4\text{-5}$ at higher temperatures (523–573 K) were measured by the GC pulse method (9) using helium (10 $\text{cm}^3 \cdot \text{min}^{-1}$) as a carrier gas. Sorbate pulses of different sizes were injected into the $\text{AlPO}_4\text{-5}$ column [o.d., 3 mm; i.d., 2 mm, and length, 17 cm (for pyridine pulse experiments); length, 51 cm (for the pulse experiments for other sorbates)] at a known temperature and the elution chromatogram of each pulse was recorded until the recorder pen reached the baseline. The detailed experimental arrangement and procedures for the pulse experiments have been given in previous papers (10, 11).

Heats of sorption of *n*-hexane, cyclohexane, and benzene in $\text{AlPO}_4\text{-5}$ at near zero intracrystalline sorbate concentration were determined by the GC pulse method (12) based on the variation of sorbate retention volume with temperature. The GC retention data were collected at different temperatures (483–673 K) using helium (10 $\text{cm}^3 \cdot \text{min}^{-1}$) as the carrier gas with the pulses of the sorbate vapor diluted with helium (concentration of sorbate in the pulse, about 1.0 mol%). The size of the pulse was 0.1 cm^3 . A column (o.d., 3 mm; length, 17 cm) packed with 0.42 g of $\text{AlPO}_4\text{-5}$ was used in these experiments.

All the pulse experiments for determining the sorption and heat of sorption measurements were carried out in a Perkin-Elmer Sigma 3B gas chromatograph with a flame ionization detector.

TABLE 1
Sorption Capacity of $\text{AlPO}_4\text{-5}$ (at $p/p_s = 0.4$)

Sorbate	Critical diameter ^a (nm)	Dipole moment (D)	Sorption capacity	
			($\text{cm}^3 \cdot \text{g}^{-1}$)	($\text{mmol} \cdot \text{g}^{-1}$)
Water	0.32	1.8	0.22	12.02
<i>n</i> -Hexane	0.49	0.0	0.14	1.03
Cyclohexane	0.67	0.2	0.13	1.20
Benzene	0.66	0.0	0.13	1.46
<i>p</i> -Xylene	0.66	0.0	0.13	1.04
<i>o</i> -Xylene	0.74	0.5	0.15	1.24
Isooctane	0.70	0.0	0.13	0.79
Methanol	0.45	1.7	0.15	3.61
Ethanol	0.45	1.7	0.13	2.21
<i>n</i> -Butanol	0.49	1.8	0.13	1.42

^a Critical diameters of water, *n*-hexane, cyclohexane, and benzene are taken from Ref. (14), whereas that of the other sorbates were estimated from their molecular structure.

RESULTS

Sorption Capacity

The sorption capacity of $\text{AlPO}_4\text{-5}$ for water, hydrocarbons, and alcohols (measured at 313 K in terms of their sorption at the relative pressure of 0.4) is given in Table 1 along with the critical diameter and dipole moment of the sorbate molecules. The sorption capacity for water and *n*-hexane is consistent with that reported earlier by Wilson *et al.* (13). It may be noted that the sorption capacity (expressed as the volume of liquid sorbate sorbed per gram of aluminophosphate) for the hydrocarbons and alcohols, which differ from each other widely in their dipole moments and/or critical molecular diameters, is $0.14 \pm 0.01 \text{ cm}^3 \cdot \text{g}^{-1}$. The sorption capacity for water is, however, much higher than that observed for the other sorbates.

Sorption of *n*-Hexane, Methanol, and Benzene at 313 K

Isotherms of sorption of methanol, benzene, and *n*-hexane in the aluminophosphate at 313 K are shown in Fig. 1.

Efforts were made to fit the sorption isotherm data in the Langmuir, Freundlich,

and Dubinin–Polanyi adsorption equations (14). The data for all the sorbates could not be fitted in the Langmuir equation, indicating that the sorption of methanol, benzene, and *n*-hexane in $\text{AlPO}_4\text{-5}$ is not of the Langmuir type. The sorption data for benzene and *n*-hexane could be fitted satisfactorily in the Langmuir equation, but the data for methanol could not be fitted. However, the sorption data for all these sorbates could be fitted very well in the Dubinin–Polanyi equation, as shown in Fig. 2. The total volume of sorption space (W_0) in $\text{AlPO}_4\text{-5}$, estimated from the intercept (which is $\log W_0/V_m$, where V_m is the molar volume of sorbate in liquid state) of the linear $\log q_a$ vs $[\log(p_s/p)]^2$ plot (Fig. 2), has been estimated to be 0.16, 0.14, and $0.14 \text{ cm}^3 \cdot \text{g}^{-1}$ from the sorption data of methanol, benzene, and *n*-hexane, respectively.

Sorption of *n*-Hexane, Cyclohexane, Benzene, and Pyridine at Higher Temperatures

Sorption isotherms. Isotherms of the reversible sorption of *n*-hexane, cyclohexane, benzene, and pyridine at the different temperatures are presented in Figs. 3–6. The pulse maxima method (9) was em-

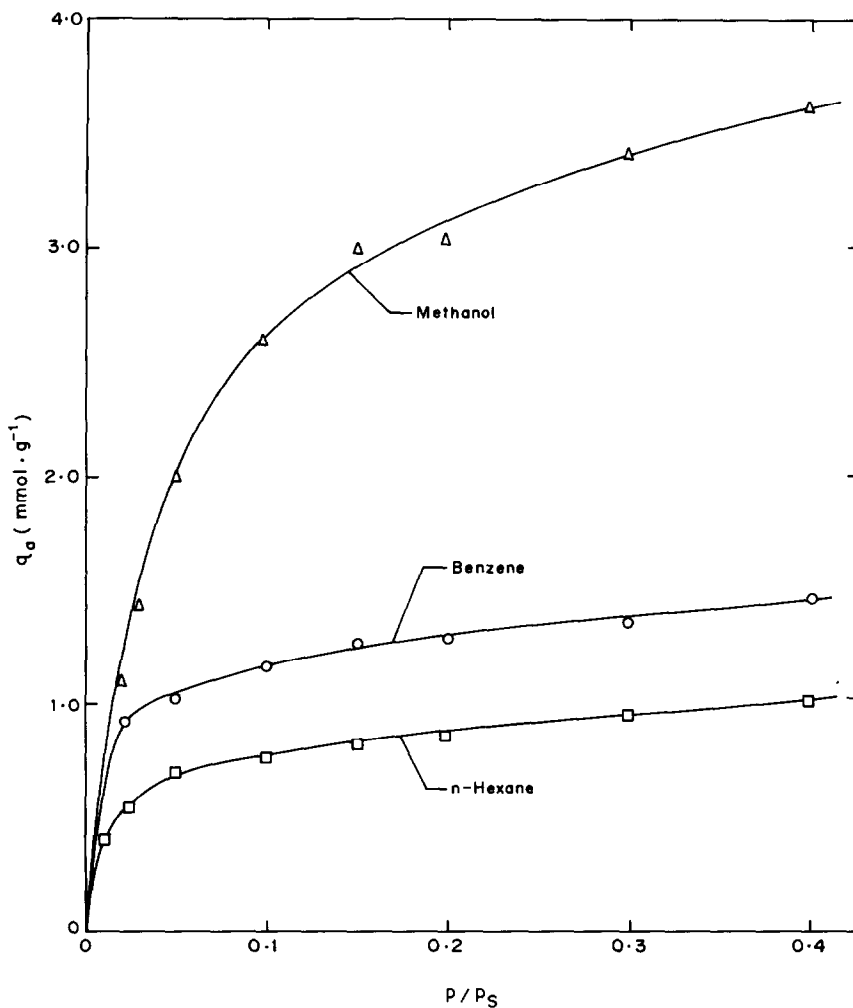


FIG. 1. Isotherms of the sorption of methanol, benzene, and *n*-hexane in $\text{AlPO}_4\text{-5}$ at 313 K.

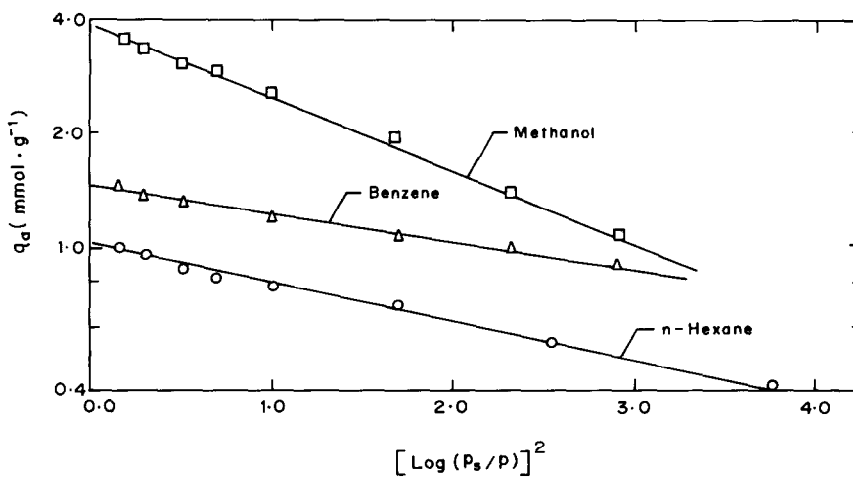


FIG. 2. Dubinin-Polanyi plots for the sorption of methanol, benzene, and *n*-hexane in $\text{AlPO}_4\text{-5}$ at 313 K.

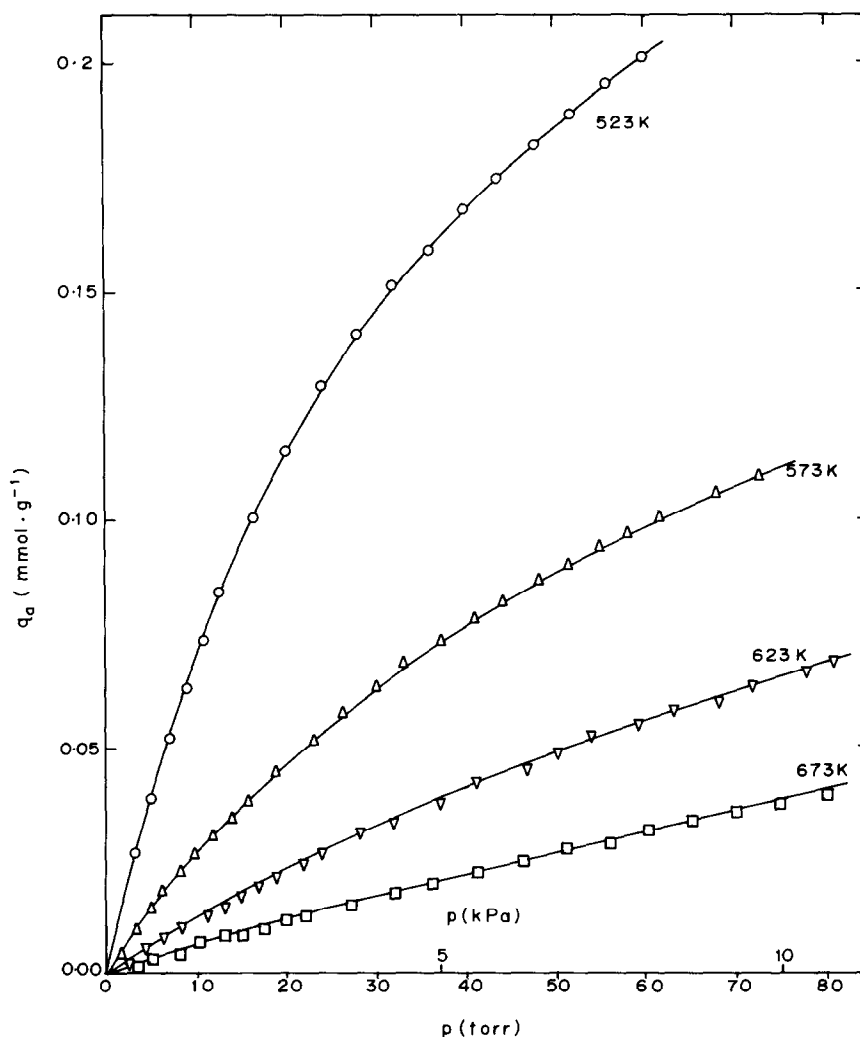


FIG. 3. Isotherms of the sorption of *n*-hexane in $\text{AlPO}_4\text{-5}$ at different temperatures.

employed for evaluating the sorption isotherms from the pulse data as the desorption edges of the elution curves for the sorbates on the aluminophosphate at all the temperatures showed a strong dependence on the amount of sorbate injected. The detailed procedure for the estimation of sorption data from superimposed elution curves by the pulse maxima method has been given elsewhere (10).

The absence of film diffusional and inter-crystalline mass transfer effects on the sorption is confirmed by varying the parti-

cle size of the aluminophosphate from 0.2 to 0.1 mm. It may also be noted that the peak maxima method minimizes the effect of longitudinal diffusion, convective mixing, and mass transfer and hence gives a more accurate estimate of the isotherm than the single injection method (9). The assumption in the evaluation of equilibrium sorption data from transient pulse experiments that a sorption equilibrium is always established locally between the mobile gas phase and the $\text{AlPO}_4\text{-5}$ particles is also satisfied in the present case as the time re-

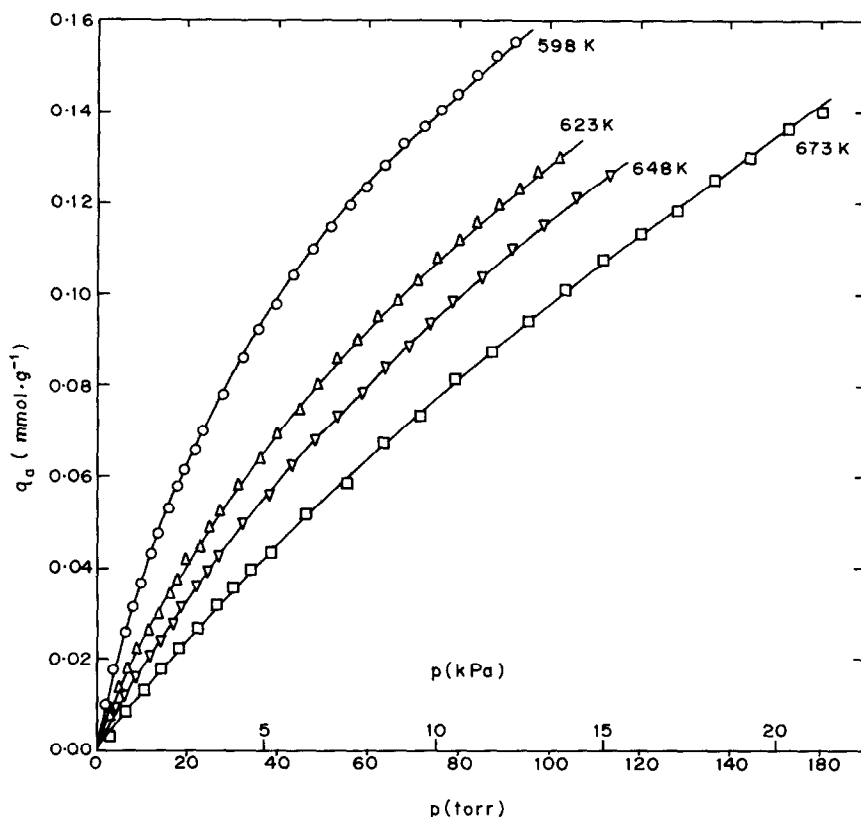


FIG. 4. Isotherms of the sorption of cyclohexane in $\text{AlPO}_4\text{-5}$ at different temperatures.

quired for the adsorption [which is estimated to be less than a microsecond for the sorption of *n*-hexane, cyclohexane, benzene, and pyridine] is extremely small as compared to the residence time of the gas flowing through the $\text{AlPO}_4\text{-5}$ particles. Here, the heat of sorption of *n*-hexane, cyclohexane, and benzene is assumed to be about $60 \text{ kJ} \cdot \text{mol}^{-1}$, and that of pyridine about $90 \text{ kJ} \cdot \text{mol}^{-1}$.

The irreversible sorption of *n*-hexane, cyclohexane, and benzene in $\text{AlPO}_4\text{-5}$ at the temperatures at which the sorption isotherms were measured was found to be absent. The irreversible sorption of pyridine at 603, 633, and 673 K was found to be 10.0, 5.0, and $2.5 \mu\text{mol} \cdot \text{g}^{-1}$, respectively.

All the data for the reversible sorption of *n*-hexane, cyclohexane, benzene, and pyridine (Figs. 3–6) fitted very well in the

Freundlich adsorption equation,

$$q_a = kp^n, \quad (1)$$

where q_a is the amount adsorbed, k is the Freundlich adsorption constant, and n is the exponent to the sorbate pressure. The sorption data for benzene at 523 K could be fitted satisfactorily in the Dubinin–Polanyi equation. However, no attempt was made to fit the data for benzene at higher temperatures or the data for other sorbates since their sorption temperatures were very close to or higher than the critical temperatures of the corresponding sorbate. Efforts were also made to fit the sorption data for all the sorbates in the Langmuir adsorption equation but these were without success.

The Freundlich parameters (k and n) for the sorption of *n*-hexane, cyclohexane, benzene, and pyridine are presented in Ta-

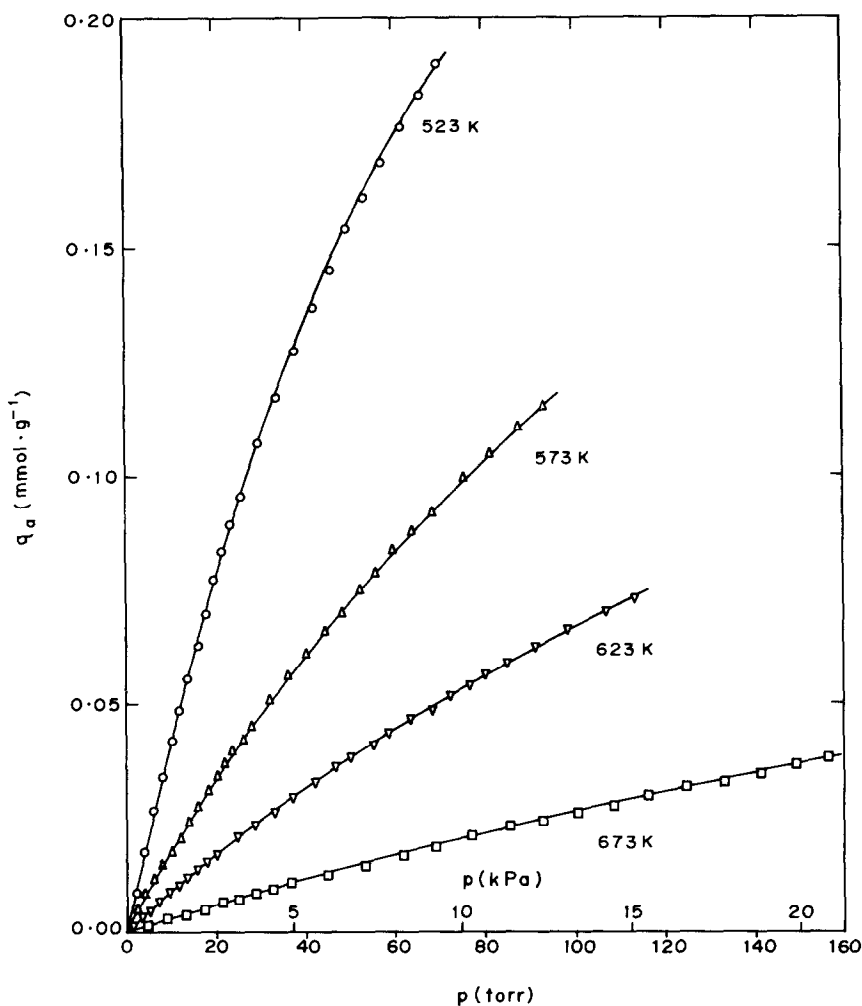


FIG. 5. Isotherms of the sorption of benzene in $\text{AlPO}_4\text{-5}$ at different temperatures.

ble 2. Figure 7 shows the temperature dependence of Freundlich sorption constant (k) for the different sorbates; for all the sorbates, $\ln k$ is inversely proportional to the sorption temperature, thus satisfying on Arrhenius-type equation. The exponent to the sorbate pressure (n) is expected to be independent of temperature. However, the results (Table 2) indicate a small increase in the value of n for all the sorbates with the increase in the sorption temperature.

Isosteric heat of sorption. Figure 8 shows the dependence of the isosteric heat of sorption (Q_a) of *n*-hexane, cyclohexane, benzene, and pyridine in $\text{AlPO}_4\text{-5}$ on the

sorbate loading in the aluminophosphate. The isosteric heat of sorption at the different intracrystalline sorbate concentrations was evaluated from the sorption isotherm data (Figs. 3–6) by means of the Clausius–Clapyron equation (14).

It is interesting to note from Fig. 8 that the heat of sorption of pyridine, *n*-hexane, and cyclohexane is strongly influenced by the sorbate loading, particularly at the higher sorbate loadings, whereas the influence of sorbate loading on the heat of benzene sorption is very weak. In the case of sorption of *n*-hexane and pyridine, Q_a increases with the increase in the sorbate

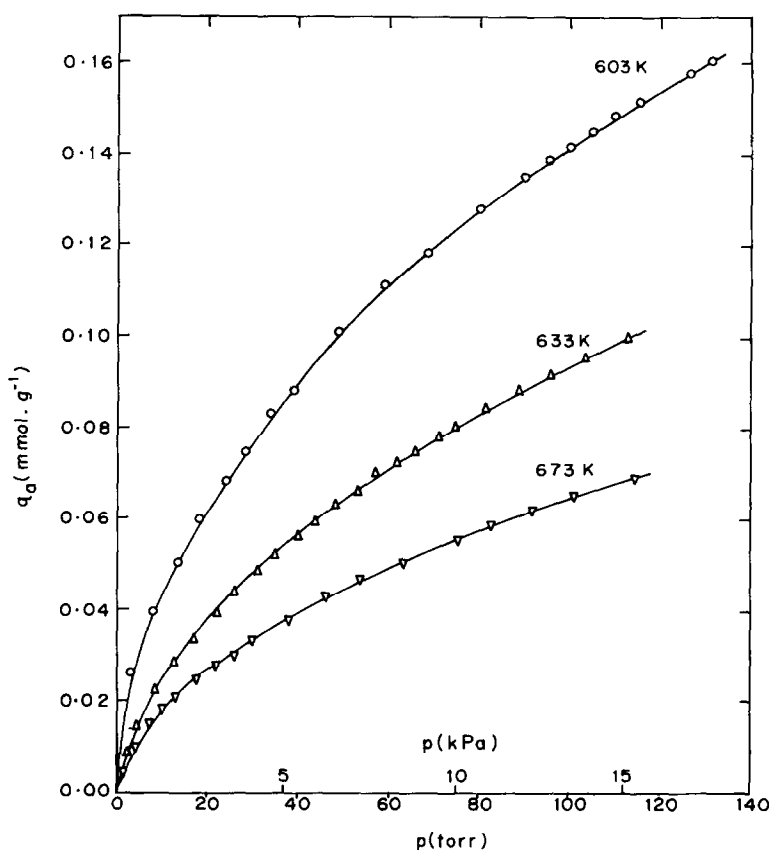
FIG. 6. Isotherms of the sorption of pyridine in $\text{AlPO}_4\text{-5}$ at different temperatures.

TABLE 2

Freundlich Parameters for Sorption of *n*-Hexane, Cyclohexane, Benzene, and Pyridine in $\text{AlPO}_4\text{-5}$

Sorbate	Temperature (K)	$k \times 10^6$ ($\text{gmol} \cdot \text{g}^{-1} \cdot \text{Torr}^{-1}$)	n
<i>n</i> -Hexane	523	15.58	0.70
	573	4.78	0.75
	623	1.97	0.82
	673	0.90	0.86
Cyclohexane	598	8.07	0.70
	623	4.80	0.74
	648	3.04	0.81
	673	2.07	0.84
Benzene	523	6.61	0.82
	573	2.75	0.84
	623	1.35	0.86
	673	0.47	0.88
Pyridine	603	13.57	0.51
	633	6.77	0.58
	673	4.24	0.60

loading. In contrast, the heat of sorption of cyclohexane decreases with the increase in the sorbate loading. It may also be noted that the heats of sorption of *n*-hexane, cyclohexane, and benzene are of comparable values at the lower sorbate loadings but differ from each other in a more and more significant manner at the higher sorbate loadings. At the sorbate loading of $0.1 \text{ mmol} \cdot \text{g}^{-1}$, the heat of sorption of these sorbates is in the following order: pyridine $\geq n$ -hexane $>$ benzene $>$ cyclohexane.

Heat of sorption by GC pulse technique. The heat of sorption of *n*-hexane, cyclohexane, and benzene in $\text{AlPO}_4\text{-5}$ at near zero sorbate loading was determined from the GC pulse retention data obtained at the different temperatures using the relation (12)

$$\log(V_R) = \alpha - (\Delta H/2.303R)(1/T), \quad (2)$$

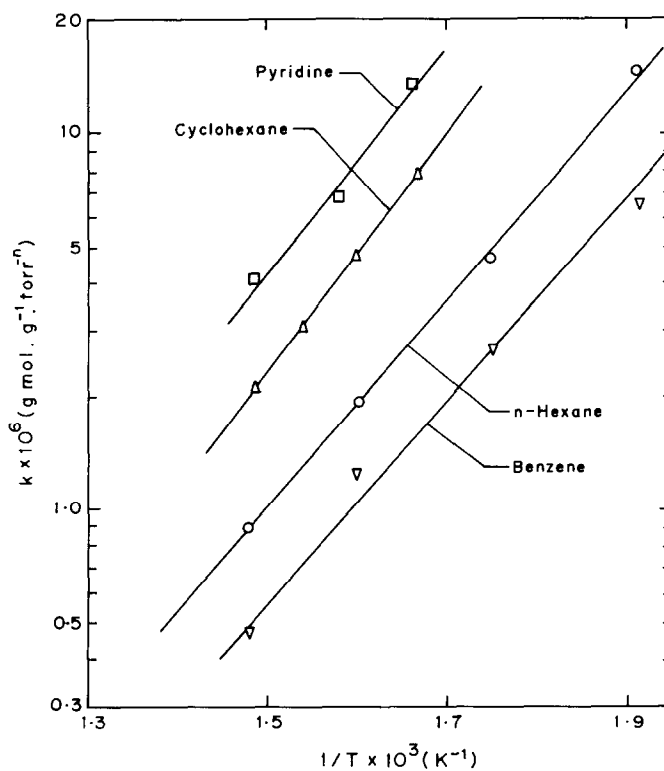


FIG. 7. Temperature dependence of Freundlich sorption constant (k).

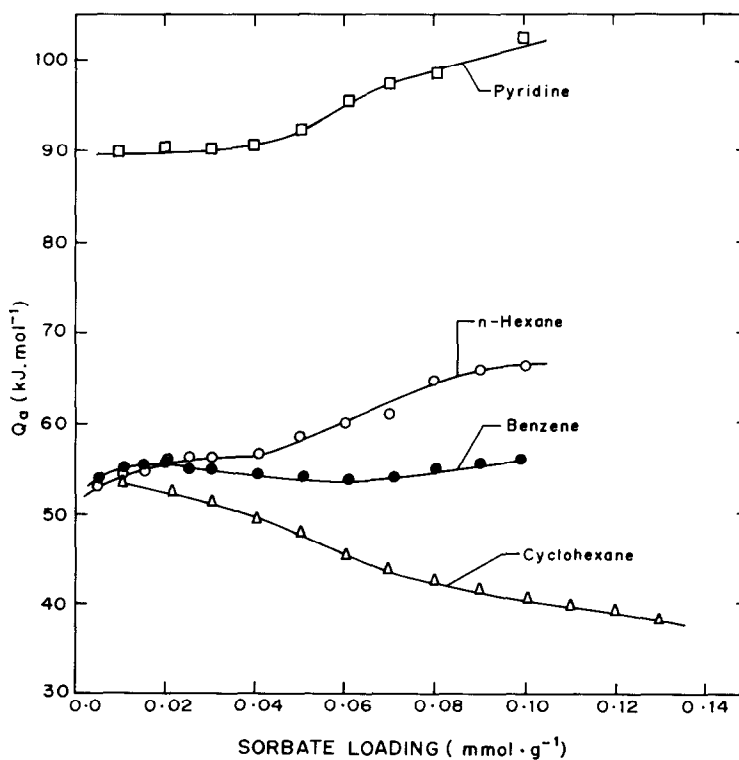


FIG. 8. Variation of isosteric heat of sorption (Q_a) of *n*-hexane, cyclohexane, benzene, and pyridine in $\text{AlPO}_4\text{-5}$ with the sorbate loading.

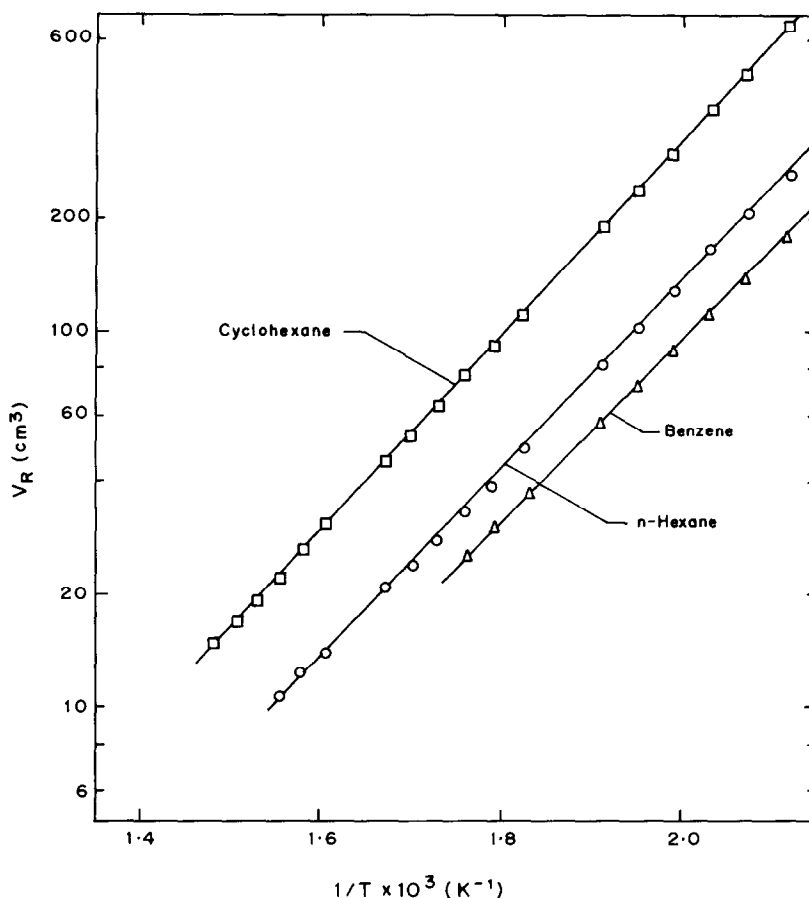


FIG. 9. Log V_R vs $1/T$ plots according to Eq. (2) for determining the heats of sorption of *n*-hexane, cyclohexane, and benzene in $\text{AlPO}_4\text{-5}$ by the GC pulse technique.

where V_R is the retention volume of sorbate, which is equal to $(t_m - t_d) \cdot V$; t_m and t_d are the retention times for sorbate and non-sorbate, respectively; V is the carrier gas flow rate (corrected for the column conditions); ΔH is the heat of sorption; R is the gas constant; T is the temperature; and α is a constant.

The values of the heat of sorption (ΔH) of the sorbates, obtained from the slopes of the linear plots of $\log V_R$ vs $1/T$, shown in Fig. 9, are as follows.

Sorbate:	<i>n</i> -Hexane	Cyclohexane	Benzene
$-\Delta H$ (kJ · mol ⁻¹):	50.1	51.0	49.9

The results indicate that the values of the heat of sorption of the sorbates at near zero

sorbate loading are close to each other and also to the isosteric heat of sorption of the sorbates at the lower sorbate loadings (Fig. 8).

In order to obtain a reliable value of the heat of adsorption by the GC pulse method, the condition that the adsorbate concentration falls essentially in the linear portion of the isotherm must be satisfied (15). This was accomplished in the pulse experiments of *n*-hexane, cyclohexane, and benzene by using a very small and dilute sorbate pulse (pulse size, 0.1 cm³; sorbate concentration, 1 mol%) and was confirmed by the observation that the carrier gas flow rate had no effect on the retention volume of the sorbate. However, it was not possible to col-

lect pyridine pulse data by satisfying the above condition because of the highly non-linear nature of the pyridine sorption isotherm (Fig. 6), even at a very low sorbate concentration.

Free energy and entropy changes in sorption. The thermodynamic data for the sorption of *n*-hexane, cyclohexane, benzene, and pyridine in $\text{AlPO}_4\text{-5}$ at different sorbate loadings and temperatures are presented in Tables 3–6. The data were evaluated from the sorption isotherm data (Figs. 3–6) using the following relations,

$$\Delta G = -RT \ln P/p \quad (3)$$

$$\Delta G = \Delta H - T\Delta S \quad (4)$$

$$S_a = S_g + \Delta S, \quad (5)$$

where ΔG , ΔH (which is equal to isosteric heat of sorption under isothermal conditions, neglecting gas imperfections), and ΔS are the standard free energy, enthalpy, and entropy changes in the sorption process, respectively; S_g is the entropy of sorbate vapor at the standard pressure P ; S_a is the entropy of sorbed phase; and P and p

are the equilibrium pressures of the sorbate phase in a standard state and the state at which the studies were conducted, respectively. The standard state pressure (P) is taken as 760 Torr. The values of S_g for the various sorbates were taken from the data given elsewhere (16).

The results (Tables 3–6) reveal that, in the sorption of *n*-hexane, cyclohexane, benzene, and pyridine, the free energy change ($-\Delta G$) decreases with the increase in the sorbate loading and the temperature, whereas the entropy change ($-\Delta S$) shows a variation with sorbate loading, but is more or less independent of the sorption temperature. For the sorption of *n*-hexane, benzene, and pyridine, S_a , and consequently the mobility of the sorbed phase, tend to decrease with the sorbate loading and increase with the temperature. However, in the case of the cyclohexane sorption, S_a increases not only with the temperature but also with the sorbate loading.

Figure 10 shows a comparison between the observed entropy change ($-\Delta S_m$) associated with the sorption (after correcting for the contributions for the entropy change in

TABLE 3
Thermodynamic Data for the Sorption of *n*-Hexane in $\text{AlPO}_4\text{-5}$

Amount sorbed, q_a (mmol · g ⁻¹)	Temperature (K)	$-\Delta G$ (kJ · mol ⁻¹)	$-\Delta S$ (J · K ⁻¹ · mol ⁻¹)	S_g (J · K ⁻¹ · mol ⁻¹)	S_a (J · K ⁻¹ · mol ⁻¹)
0.02	523	26.0	56.5	489.0	432.5
	573	22.5	57.7	510.4	452.7
	623	19.7	57.6	531.4	473.8
	673	17.3	56.8	552.3	495.5
0.04	523	22.0	66.1	489	422.9
	573	18.4	66.7	510.4	443.7
	623	15.4	66.1	531.4	465.2
	673	12.7	65.2	552.3	487.1
0.06	523	20.0	76.7	489.5	412.8
	573	15.8	77.2	510.4	433.2
	623	12.7	75.9	531.4	455.5
0.08	523	18.3	87.4	489.5	402.1
	573	13.8	87.8	510.4	422.6
0.10	523	16.8	95.2	489.5	394.3
	573	12.0	95.2	510.4	415.2

TABLE 4
Thermodynamic Data for the Sorption of Cyclohexane in $\text{AlPO}_4\text{-5}$

Amount sorbed, q_a ($\text{mmol} \cdot \text{g}^{-1}$)	Temperature (K)	$-\Delta G$ ($\text{kJ} \cdot \text{mol}^{-1}$)	$-\Delta S$ ($\text{J} \cdot \text{K}^{-1} \cdot \text{mol}^{-1}$)	S_g ($\text{J} \cdot \text{K}^{-1} \cdot \text{mol}^{-1}$)	S_a ($\text{J} \cdot \text{K}^{-1} \cdot \text{mol}^{-1}$)
0.02	598	25.1	50.0	410.0	360.0
	623	23.7	50.2	418.4	368.2
	648	23.0	49.4	431.0	381.6
	673	21.7	49.5	439.3	389.8
0.04	598	21.2	47.4	410.0	362.6
	623	19.0	49.1	418.4	369.3
	648	18.5	47.9	431.0	383.1
	673	17.3	47.9	439.3	391.4
0.06	598	18.5	44.5	410.0	365.5
	623	16.4	46.1	418.4	372.3
	648	15.8	45.1	431.0	385.9
	673	14.7	45.1	439.3	394.2
0.08	598	16.3	43.8	410.0	366.2
	623	14.3	45.4	418.4	373.0
	648	13.8	44.4	431.0	386.6
	673	12.8	44.2	439.3	395.2
0.10	598	14.6	43.4	410.0	366.6
	623	12.6	44.9	418.4	373.5
	648	12.1	43.8	431.0	387.2
	673	11.2	43.5	439.3	395.8
0.12	598	13.0	43.5	410.0	366.5
	623	11.1	44.8	418.4	373.6
	648	10.7	43.7	431.0	387.3
	673	10.0	43.2	439.3	396.1

TABLE 5
Thermodynamic Data for the Sorption of Benzene in $\text{AlPO}_4\text{-5}$

Amount sorbed, q_a ($\text{mmol} \cdot \text{g}^{-1}$)	Temperature (K)	$-\Delta G$ ($\text{kJ} \cdot \text{mol}^{-1}$)	$-\Delta S$ ($\text{J} \cdot \text{K}^{-1} \cdot \text{mol}^{-1}$)	S_g ($\text{J} \cdot \text{K}^{-1} \cdot \text{mol}^{-1}$)	S_a ($\text{J} \cdot \text{K}^{-1} \cdot \text{mol}^{-1}$)
0.02	523	22.0	63.2	330.5	267.3
	573	20.3	60.6	345.2	284.6
	623	17.8	59.7	355.6	295.9
	673	13.3	62.0	370.3	308.3
0.04	523	19.0	67.1	330.5	263.4
	573	16.4	65.8	345.2	279.4
	623	13.9	64.5	355.6	291.1
	673	8.7	67.4	370.3	302.9
0.06	523	17.2	66.7	330.5	263.8
	573	14.1	66.2	345.2	279.0
	623	11.2	65.5	355.6	290.1
0.08	523	13.2	75.8	330.5	254.7
	573	12.4	75.3	345.2	269.9
0.10	523	14.6	80.1	330.5	250.4
	573	11.0	79.5	345.2	265.7

TABLE 6
Thermodynamic Data for the Sorption of Pyridine in $\text{AlPO}_4\text{-5}$

Amount sorbed, q_a (mmol · g ⁻¹)	Temperature (K)	$-\Delta G$ (kJ · mol ⁻¹)	$-\Delta S$ (J · K ⁻¹ · mol ⁻¹)	S_g (J · K ⁻¹ · mol ⁻¹)	S_a (J · K ⁻¹ · mol ⁻¹)
0.02	603	30.0	99.7	359.8	260.1
	633	24.8	103.1	368.2	265.1
	673	23.4	99.1	378.7	279.6
0.04	603	22.4	114.0	359.8	245.8
	633	18.5	114.6	368.2	253.6
	673	16.3	111.1	378.7	267.6
0.06	603	18.6	128.4	359.8	231.4
	633	15.0	128.0	368.2	240.2
0.08	603	15.8	135.6	359.8	224.2
	633	12.3	134.8	368.2	233.4
0.10	603	13.73	146.4	359.8	213.4
	633	10.14	145.1	368.2	223.1

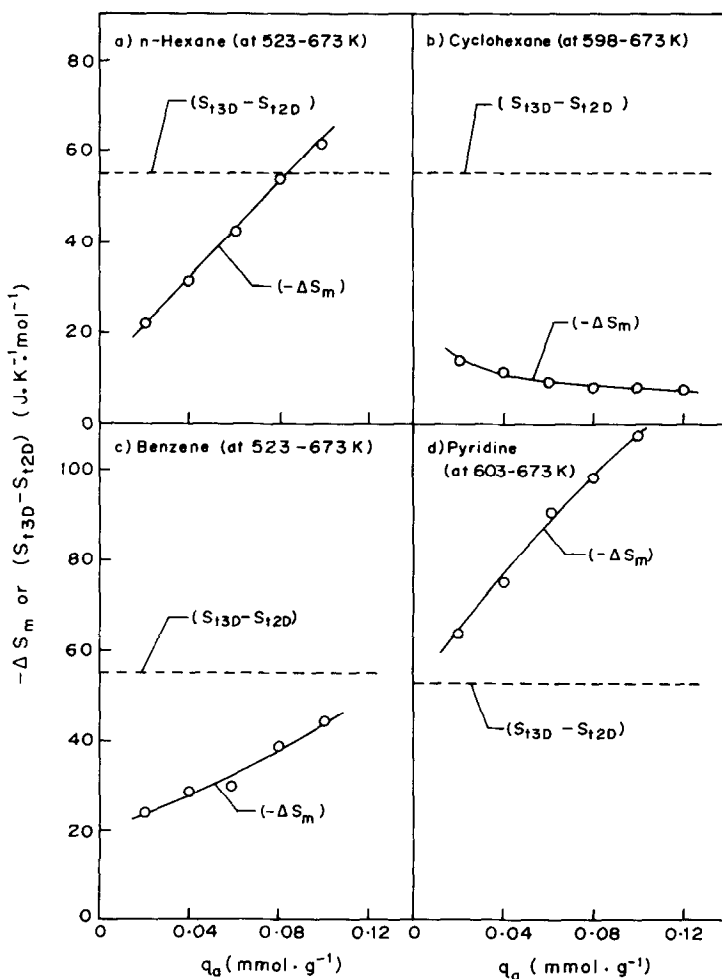


FIG. 10. Comparison between the observed entropy change ($-\Delta S_m$) at different sorbate loadings and the theoretical entropy change for mobile sorption ($S_{13D} - S_{12D}$) in the sorption of *n*-hexane, cyclohexane, benzene, and pyridine in $\text{AlPO}_4\text{-5}$.

TABLE 7

Theoretical Entropy Changes in the Mobile and Localized Sorption of *n*-Hexane, Cyclohexane, Benzene, and Pyridine

Sorbate	Temperature (K)	S_{3D} (J · K ⁻¹ · mol ⁻¹)	S_{2D} (J · K ⁻¹ · mol ⁻¹)	Entropy change (J · K ⁻¹ · mol ⁻¹)	
				Mobile sorption ($S_{3D} - S_{2D}$)	Localized sorption (S_{3D})
<i>n</i> -Hexane	523	176.0	121.9	54.1	176.0
	573	177.9	123.4	54.5	177.9
	623	179.6	124.7	54.9	179.6
	673	181.2	126.0	55.2	181.2
Cyclohexane	598	178.5	123.9	54.6	178.5
	623	179.3	124.4	54.9	179.3
	648	180.1	125.2	54.9	180.1
	673	180.9	125.8	55.1	180.9
Benzene	523	174.8	121.1	53.7	174.8
	573	176.7	122.2	54.5	176.7
	623	178.4	124.0	54.4	178.4
	673	180.0	125.2	54.8	180.0
Pyridine	603	177.9	125.0	52.9	177.9
	633	178.9	125.8	53.1	178.9
	673	180.2	126.8	53.4	180.2

the vapor phase and in the sorbed phase) at the different sorbate loadings and the theoretical entropy change ($S_{3D} - S_{2D}$) (where, S_{3D} and S_{2D} are the translational entropies of the three-dimensional and two-dimensional sorbate vapors, respectively) for the mobile film model (17) in the sorption of *n*-hexane, cyclohexane, benzene, and pyridine.

The results reveal that when the sorbate loading is increased, the entropy change ($-\Delta S_m$) in the sorption of *n*-hexane, benzene, and pyridine increases but that of cyclohexane decreases. Also, for the sorption of *n*-hexane (at lower sorbate loadings, $q_a < 0.08$ mmol · g⁻¹), cyclohexane, and benzene, the observed entropy change is much smaller than the theoretical value. In the case of the pyridine sorption, the observed entropy change is higher than the theoretical entropy change.

The values of the translational entropies of the three-dimensional and two-dimensional vapors of the sorbates at different temperatures are given in Table 7. These

values were obtained from the expressions (17, 18)

$$S_{3D} = R \ln(M^{1.5} \cdot T^{2.5}) - 9.61 \quad (6)$$

and

$$S_{2D} = 0.667 S_{3D} + 2.76 \ln T - 12.71, \quad (7)$$

where M is the molecular weight (the values of S_{3D} and S_{2D} are expressed in J · K⁻¹ · mol⁻¹). The change of entropy in the sorption for the mobile and localized sorption models (with no loss of rotational degrees of freedom of sorbed molecules) is expected to be equal to ($S_{3D} - S_{2D}$) and S_{3D} , respectively. The values of the entropy change for the two sorption models are included in Table 7. It may be noted that although the S_{3D} and S_{2D} increase with temperature (the increase, however, is small), ($S_{3D} - S_{2D}$), and consequently the entropy change in the mobile sorption, is almost independent of temperature.

ΔS_m values, at the different sorbate loadings, were obtained from observed ΔS , av-

eraged over the sorption temperature range, using the relation (17)

$$\Delta S_m = \Delta S + R \ln(A^*/A), \quad (8)$$

where A^* is the standard molecular area (equal to $4.08 T \times 10^{-16} \text{ cm}^2$) and A is the molecular area of the sorbate, calculated from the density of the sorbate liquid using the relation suggested by Emmett and Brunauer (19).

DISCUSSION

Low-Temperature Sorption

The sorption capacity of $\text{AlPO}_4\text{-5}$ for all the sorbates (except water) at the relative pressure of 0.4 has been found to be about $0.14 \text{ cm}^3 \cdot \text{g}^{-1}$ and this is very close to the values reported by Wilson *et al.* (13) for the sorption of oxygen ($0.15 \text{ cm}^3 \cdot \text{g}^{-1}$), *n*-hexane ($0.14 \text{ cm}^3 \cdot \text{g}^{-1}$), cyclohexane ($0.14 \text{ cm}^3 \cdot \text{g}^{-1}$), and neopentane ($0.14 \text{ cm}^3 \cdot \text{g}^{-1}$). The sorption capacity for nitrogen (at 78 K relative pressure of 0.3) has also been found to be about $0.16 \text{ cm}^3 \cdot \text{g}^{-1}$ (6). The sorption capacity for water ($0.22 \text{ cm}^3 \cdot \text{g}^{-1}$) is much higher than that for the other sorbates. The difference in the sorption capacities for water and the other sorbates is attributable (2) to the presence of both the large-pore voids (cylindrical channels formed by 12-membered rings parallel to the *c*-axis) and the small-pore voids (columns of twisted chains of 4- and 6-membered rings parallel to the *c*-axis) in the structure of $\text{AlPO}_4\text{-5}$. The small-pore voids are accessible only to water molecules because of their very small kinetic diameter (0.265 nm), whereas the large-pore voids are easily accessible to all the sorbates. It is interesting to note that although the cylindrical channels in $\text{AlPO}_4\text{-5}$ are polar, its sorption capacity is not strongly influenced by the polarity (or dipole moment) of sorbate molecules. It may also be noted that the sorption capacity (except for water) is not affected by the configuration and/or critical molecular size of the sorbates.

The fitting of the low-temperature (313

K) sorption isotherm data for methanol, benzene, and *n*-hexane in the Dubinin–Polanyi equation (Fig. 2) indicates that their sorption in $\text{AlPO}_4\text{-5}$ occurs by the volume filling mechanism. The total volume of sorption space in $\text{AlPO}_4\text{-5}$ is estimated to be $0.14 \text{ cm}^3 \cdot \text{g}^{-1}$ from the sorption of *n*-hexane and benzene, and $0.16 \text{ cm}^3 \cdot \text{g}^{-1}$ from the sorption of methanol. The observed small difference in the sorption space probably arises from the differences in the bulk liquid density of the sorbate (which is used in the calculation of sorption space) and its actual density in the channel of $\text{AlPO}_4\text{-5}$ at the saturation. The two densities are expected to be somewhat different since the molecular size of the sorbates is quite comparable to the channel diameter and also since the sorbate molecules in the channels are subjected to large surface tension forces. Dubinin *et al.* (20) observed that the density of polar substances sorbed in zeolite micropores at the saturation exceeds that of the liquid owing to the closer packing of the polar molecules in the zeolite than in the corresponding liquid, but in the case of the nonpolar sorbates the density in the sorbed state is somewhat lower than that in the liquid state. This may be the reason for the higher sorption space obtained from the methanol sorption data and also for the observed higher sorption capacity for *o*-xylene than that for *p*-xylene.

High-Temperature Sorption

The sorption of *n*-hexane (at 523–673 K), cyclohexane (at 598–673 K), benzene (at 523–673 K), and pyridine (at 603–673 K) in $\text{AlPO}_4\text{-5}$ follows the Freundlich sorption isotherm. The fact that the sorption data could not be fitted in the Langmuir model indicates the absence of ideal localized sorption of the sorbates in the aluminophosphate.

The isosteric heat of sorption of benzene in $\text{AlPO}_4\text{-5}$ is influenced by the sorbate loading only to a small extent, but for the other sorbates, it is strongly dependent on the sorbate loading. The increase in the iso-

steric heat of sorption of pyridine and *n*-hexane with the increase in the sorbate loading shows the presence of attractive interactions between the sorbed molecules. The decrease in the isosteric heat of sorption of cyclohexane with the sorbate loading, however, is expected to be due to the repulsive interaction between the sorbed molecules.

The values of isosteric heat of sorption of *n*-hexane, benzene, and cyclohexane at the lower sorbate loadings are close to each other, as are the values of the heat of sorption of these sorbates measured by the GC pulse method. Further, a comparison of the values of the isosteric heat of sorption extrapolated to zero sorbate loading (Fig. 8), obtained from the sorption isotherm data, with those at near zero sorbate loading obtained with the GC pulse method shows that there is very good agreement among the heats of sorption of *n*-hexane, benzene, and cyclohexane as measured by the two methods.

The heat of sorption of pyridine is much higher than that observed for the other sorbates. The higher heat of sorption of pyridine is mainly attributable to its very high molecular polarity (dipole moment of pyridine in gas phase, 4.37 D). Since the channels of $\text{AlPO}_4\text{-5}$ are polar, their interaction with the polar sorbate molecules is expected to result in a much higher heat of sorption than that expected from their interaction with the nonpolar sorbate molecules, such as *n*-hexane and benzene.

The comparison of the observed entropy change ($-\Delta S_m$) with the theoretical one predicted for the mobile and localized film models (Fig. 10 and Table 7) clearly shows that the sorption of *n*-hexane, cyclohexane, benzene, and pyridine in $\text{AlPO}_4\text{-5}$ at the higher temperatures (523–673 K) is mobile. The mobility of sorbed molecules is, however, strongly dependent on the sorbate loading. It increases in the sorption of cyclohexane and decreases in the sorption of *n*-hexane, benzene, and pyridine, with the increase in the sorbate loading.

In the sorption of *n*-hexane (for $q_a < 0.08$ mmol \cdot g $^{-1}$), benzene, and cyclohexane, the observed entropy change is much less than the theoretical value expected for the mobile sorption (i.e., the sorption with a complete loss of the degree of translation). This implies that, in these cases the degree of translation normal to the surface is converted into a vibration and the entropy associated with the vibration normal to surface is quite appreciable. For example, at the sorbate loading of 0.02 mmol \cdot g $^{-1}$, the entropies of vibration of sorbed *n*-hexane, cyclohexane, and benzene are found to be 32.2, 41.3, and 29.8 K \cdot k $^{-1}$ \cdot mol $^{-1}$, respectively, and the frequencies of vibration of these molecules and the wavelengths of the undulatory motion or vibratory flight resulting from the vibration, estimated by the procedure given by de Boer (21), have been found to be about 7.3×10^{11} , 2.6×10^{11} , and 9.6×10^{11} s $^{-1}$ and 0.53, 1.54, and 0.42 nm, respectively. It may be noted that the wavelength of the vibratory flight of the sorbed molecules in the channels is somewhat greater than the atomic distances of the aluminophosphate; in the case of cyclohexane sorption, it is even greater than the channel diameter. Thus, in addition to the unrestricted freedom of movement in two directions along the surface, the mobility of these sorbate molecules in the channels of $\text{AlPO}_4\text{-5}$ is greatly enhanced by their vibratory flight. For such cases, Kemball (18) has introduced the term "supermobile sorption."

Although the sorption of *n*-hexane of higher sorbate loading ($q_a > 0.08$ mmol \cdot g $^{-1}$) and pyridine is also described by the mobile film model, the observed entropy change in these cases is greater than the one predicted for the model. This shows that the two-dimensional translational motion parallel to the surface is itself somewhat restricted. The entropy change in addition to that entailed by the loss of one degree of translation reveals that some of the rotational degrees of freedom of the sorbed molecules are lost. It is to be noted

here that the restriction on the rotation of sorbed pyridine increases to a large extent and consequently its mobility decreases with the increase in the sorbate loading.

CONCLUSIONS

The following conclusions have been drawn from the present investigation.

(i) The sorption capacity values of $\text{AlPO}_4\text{-5}$ (measured in terms of the volume of liquid sorbate per gram of the adsorbent) for the various sorbates (except water) are close to each other (about $0.14 \text{ cm}^3 \cdot \text{g}^{-1}$) although their dipole moments and critical molecular sizes differ widely from each other.

(ii) The sorption of methanol, *n*-hexane, and benzene at 313 K occurs by the volume filling mechanism, thus satisfying the Dubinin–Polanyi equation; the total volume of sorption space in $\text{AlPO}_4\text{-5}$ is estimated to be about $0.14 \text{ cm}^3 \cdot \text{g}^{-1}$.

(iii) At higher temperatures (523–673 K), the reversible sorption of *n*-hexane, cyclohexane, benzene, and pyridine in $\text{AlPO}_4\text{-5}$ follows the Freundlich sorption isotherm. Pyridine is sorbed irreversibly to a very small extent but the other sorbates undergo only reversible sorption.

(iv) The isosteric heat of sorption of *n*-hexane, cyclohexane, and pyridine is strongly influenced by the sorbate loading, whereas that of benzene is only slightly affected by it. The variation of the heat of sorption with the sorbate loading indicates that the interactions between the sorbed molecules are attractive in the sorption of pyridine and *n*-hexane, but repulsive in the sorption of cyclohexane. The heat of sorption of pyridine is found to be much higher than that of the other sorbates, mainly because of its very high molecular polarity which causes a strong dipole–dipole interaction with the polar channels of $\text{AlPO}_4\text{-5}$. The values of the isosteric heat of sorption (obtained from the sorption isotherm) at a very low sorbate loading and at a near zero sorbate loading obtained by the GC pulse

method for *n*-hexane, cyclohexane, and benzene are very close to each other. There is also very good agreement between the values obtained by the two methods.

(v) The analysis of the entropy change in the sorption has indicated that the sorption of *n*-hexane (at lower sorbate loadings), cyclohexane, and benzene in $\text{AlPO}_4\text{-5}$ is supermobile, whereas although the sorption of *n*-hexane at a higher sorbate loading and of pyridine is also mobile, the two-dimensional translational motion of the sorbed molecules is restricted to some extent because of the loss of some of their rotational degrees of freedom. The mobility of sorbed *n*-hexane, benzene, and pyridine decreases but that of cyclohexane increases with the increase in the sorbate loading.

REFERENCES

1. Wilson, S. T., Lok, B. M., Messina, C. A., Cannan, T. R., and Flanigen, E. M., *J. Amer. Chem. Soc.* **104**, 1146 (1982).
2. Wilson, S. T., Lok, B. M., Messina, C. A., Cannan, T. R., and Flanigen, E. M., *ACS Symp. Ser.* **218**, 79 (1983).
3. Bennett, J. M., Cohen, J. P., Flanigen, E. M., Pluth, J. J., and Smith, J. V., *ACS Symp. Ser.* **218**, 109 (1983).
4. Bond, G. C., Gelstrop, M. R., Sing, K. S. W., and Theocharis, C. R., *J. Chem. Soc. Chem. Commun.* **15**, 1056 (1985).
5. Choudhary, V. R., and Akolekar, D. B., *J. Catal.* **103**, 115 (1987).
6. Choudhary, V. R., Akolekar, D. B., Singh, A. P., and Sansare, S. D., *J. Catal.*, in press.
7. Nayak, V. S., and Choudhary, V. R., *Appl. Catal.* **4**, 31 (1982).
8. Choudhary, V. R., *J. Chromatogr.* **268**, 207 (1983).
9. Kipping, P. J., and Winter, D. B., *Nature (London)* **205**, 1002 (1965).
10. Sansare, S. D., Choudhary, V. R., and Doraiswamy, L. K., *J. Chem. Technol. Biotechnol. A* **33**, 140 (1983).
11. Choudhary, V. R., and Srinivasan, K. R., *J. Catal.* **102**, 289 (1986).
12. Choudhary, V. R., and Doraiswamy, L. K., *Ind. Eng. Chem. Prod. Res. Dev.* **10**, 218 (1971).
13. Wilson, S. T., Lok, B. M., Messina, C. A., and Flanigen, E. M., "Proc. 6th Intl. Zeolite. Conf., Reno, July 10–15, 1983" (D. Olson and A. Bisio, Eds.), p. 97. Butterworths, Surrey, 1983.
14. Breck, D. W., "Zeolite Molecular Sieves," p. 593. Wiley, New York, 1974.

15. Carberry, J. J., *Nature (London)* **189**, 391 (1961).
16. Stull, D. R., Westrum, E. F., and Sinke, G. C., "Chemical Thermodynamics of Organic Compounds." New York, 1969.
17. Gregg, S. J., "The Surface Chemistry of Solids," p. 74. Chapman & Hall, London, 1961.
18. Kemball, C., *Adv. Catal.* **2**, 233 (1950).
19. Emmett, P. H., and Brunauer, S., *J. Amer. Chem. Soc.* **59**, 1553 (1937).
20. Dubinin, M. M., Fomkin, A. A., Seliverstova, I. I., and Serpinsky, V. V., "Proc. 5th Intl. Conf. Zeolites, Naples, June 2-6, 1980" (L. V. C. Rees, Ed.), p. 468. Heyden, London, 1980.
21. de Boer, J. H., "Dynamic Character of Adsorption." Oxford Univ. Press, London, 1953.